ASTROBIOLOGY
Volume 7, Number 3, 2007

DOI: 10.1089/ast.2006.0112

Research Paper

Adenine Synthesis in Interstellar Space: Mechanisms of Prebiotic Pyrimidine-Ring Formation of Monocyclic HCN-Pentamers

RAINER GLASER, BRIAN HODGEN,[1] DEAN FARRELLY,[2] and ELLIOT McKEE[3]

ABSTRACT

The question whether the nucleobases can be synthesized in interstellar space is of fundamental significance in considerations of the origin of life. Adenine is formally the HCN pentamer, and experiments have demonstrated that adenine is formed under certain conditions by HCN pentamerization in gas, liquid, and condensed phases. Most mechanistic proposals invoke the intermediacy of the HCN tetramer AICN (4), and it is thought that adenine synthesis is completed by addition of the 5th HCN to 4 to form amidine 5 and subsequent pyrimidine cyclization. In this context, we have been studying the mechanism for prebiotic pyrimidine-ring formation of monocyclic HCN-pentamers with *ab initio* electronic structure theory. The calculations model gas phase chemistry, and the results primarily inform discussions of adenine synthesis in interstellar space. Purine formation requires tautomerization of 5 to the conjugated amidine 6 (via hydrogen-tunneling, thermally with H^+-catalysis, or by photolysis) or to keteneimine 7 (by photolysis). It was found that 5-(*N′*-formamidinyl)-1*H*-imidazole-4-carbonitrile (6) can serve as a substrate for *proton-catalyzed* purine formation under photolytic conditions and *N*-(4-(iminomethylene)-1*H*-imidazol-5(4*H*)-ylidene)formamidine (7) can serve as a substrate for *uncatalyzed* purine formation under photolytic conditions. The absence of any sizeable activation barrier for the cyclization of 7 to the (*Z*)-imino form of 9*H*-adenine (*Z*)-2 is quite remarkable, and it is this feature that allows for the formation of the purine skeleton from 7 without any further activation. Key Words: RNA—DNA—Adenine Synthesis—Gas Phase Chemistry—*Ab initio* Theory. Astrobiology 7, 455–470.

INTRODUCTION

ADENINE IS FORMALLY the pentamer of hydrocyanic acid (prussic acid), HCN, or its isomer hydroisocyanic acid, HNC, and it has been thought since the pioneering experiments by Miller and Urey (1959) and Ponnamperuma *et al*. (1963) that adenine is also formed by HCN pentamerization (Fig. 1). An "adenine synthesis" is any reaction that leads to adenine itself, **1**, or any

Department of Chemistry, University of Missouri-Columbia, Columbia, Missouri.
[1]Current address: Creighton University, Omaha, Nebraska.
[2]Current address: School of Chemistry, University of Manchester, Manchester, UK.
[3]Current address: Saint Louis University, School of Medicine, St. Louis, Missouri.

of its tautomers, (*Z*)-**2** and (*E*)-**2**, or to their respective 7*H*-tautomers. A non-aqueous path for adenine synthesis by HCN pentamerization was suggested as early as 1962 by Kliss and Matthews (1962), and at the same time by Oro (Oro, 1961; Oro and Kimball, 1962). Oro demonstrated adenine formation in refluxing ammonium cyanide solutions. In 1966, Sanchez, Ferris, and Orgel (1966) suggested HCN pentamerization in eutectic frozen solutions as a path for prebiotic adenine synthesis; the reinvestigation by Schwartz, Joosten, and Voet (1982) established this reaction as a low-yield path to adenine. The Miller group demonstrated adenine formation in frozen solutions of ammonium cyanide (Levy *et al.*, 2000) and reported kinetic studies of the effects of catalysis and temperature (Borquez *et al.*, 2005). The mechanistic proposals all agree essentially with regard to the formation of the HCN tetramer diaminomaleonitrile (DAMN), a known and well characterized molecule (Penfold and Lipscomb, 1961). In particular, it is known (Yamada *et al.*, 1968) that DAMN can isomerize to its (*E*)-isomer diaminofumaronitrile (DAFN), which has been shown to be a substrate for photolytic cyclization to form the imidazole ring in the tautomers **3** and **4** of AICN (Sanchez *et al.*, 1967; Ferris and Orgel, 1966; Orgel, 2004; Plese and Jasien, 1996). As an alternative, Oro discussed an ammonia-catalyzed path (involving formimidamide) to AICN formation (Oro, 1961; Oro and Kimball, 1962). The addition of HCN to AICN has been demonstrated as a possible thermal route to adenine and presumably involves the HCN pentamer **5** (Sanchez *et al.*, 1968). More recently, Zubay and Mui (2001) and Hill and Orgel (2002) showed that reaction of AICN with ammonium formate (NH_4HCO_2) at elevated temperatures (*circa* 100–110 °C) leads to adenine, and this path is thought to involve AICA.

The idea of prebiotic adenine synthesis on Earth remains controversial (Shapiro, 1995). The HCN-based syntheses rely on the presence of a reducing atmosphere, and there is growing evidence that Earth did start out with a reducing atmosphere (Habicht *et al.*, 2002; Tian *et al.*, 2005). But even with the substrates present, questions remain regarding the kinetic and thermodynamic feasibilities and probabilities of adenine synthesis under various conditions on an early Earth. Exogenous delivery is another possibility (Chyba and Sagan, 1992), and extraterrestrial sources of adenine and potential adenine precursors are known to exist. Mass-spectrometric measurements during the 1986 flyby of the *Vega 1* spacecraft of comet Halley showed that the chondritic core of cometary dust particles is surrounded by an organic mantle and that adenine was among the identified heterocycles (Kissel and Krueger, 1987). Matthews (1997) argued that the brown-orange color arising from the 1994 impacts of comet P/Shoemaker-Levy 9 on Jupiter might indicate the presence of HCN polymers and that such polymers might also cause the coloration of Saturn. Matthews discussed polyaminocyanomethylenes and polyamidines; the former especially can be seen as potential precursors to adenine formation (Matthews, 1997). It is well established that large amounts of HCN and HNC occur in interstellar space (Ishii *et al.*, 2006). The distribution of these isomers in protostellar dust cores has been measured (Tennekes *et al.*, 2006), and the formation of small HCN-oligomers in interstellar clouds has been discussed (Smith *et al.*, 2001). Ghosh and Ghosh (1980, 1982) considered the role of proton-catalysis for HCN oligomerization and argued that $HCNH^+$ might be a substrate for adenine synthesis in space.

Pentamer **5** requires tautomerization before pyrimidine formation can occur from either **6** or **7**. The formamidines **5** and **6** can be interconverted via 1,3-H-shift, and such an H-shift is possible without major electronic rearrangements. On the other hand, the conversion of **5** to **7** involves a 1,5-H-shift and transforms a push-pull-stabilized heteroaromatic system into a quinoid keteneimine. Pentamers **5** to **7** allow for C=N isomerism and various C–N conformations; the structures with the capacity for cyclization to adenine are shown in Fig. 1. As can be seen, pentamer **6** might form adenine (*Z*)-**2** by amine addition to the nitrile group. Keteneimine **7** has not previously been discussed in the context of adenine synthesis (or in any other context). It is unknown whether this molecule can exist as a stable compound; nor is it known whether, and under what conditions, it might cyclize to **2**.

In this paper, we report the results of an *ab initio* study of several key issues regarding the mechanisms of pyrimidine-ring formation of isomeric monocyclic HCN-pentamers and discuss implications for adenine synthesis in interstellar space. We first examine the aminolysis reaction **6** → **2** (Fig. 2). Nucleophilic additions to nitriles

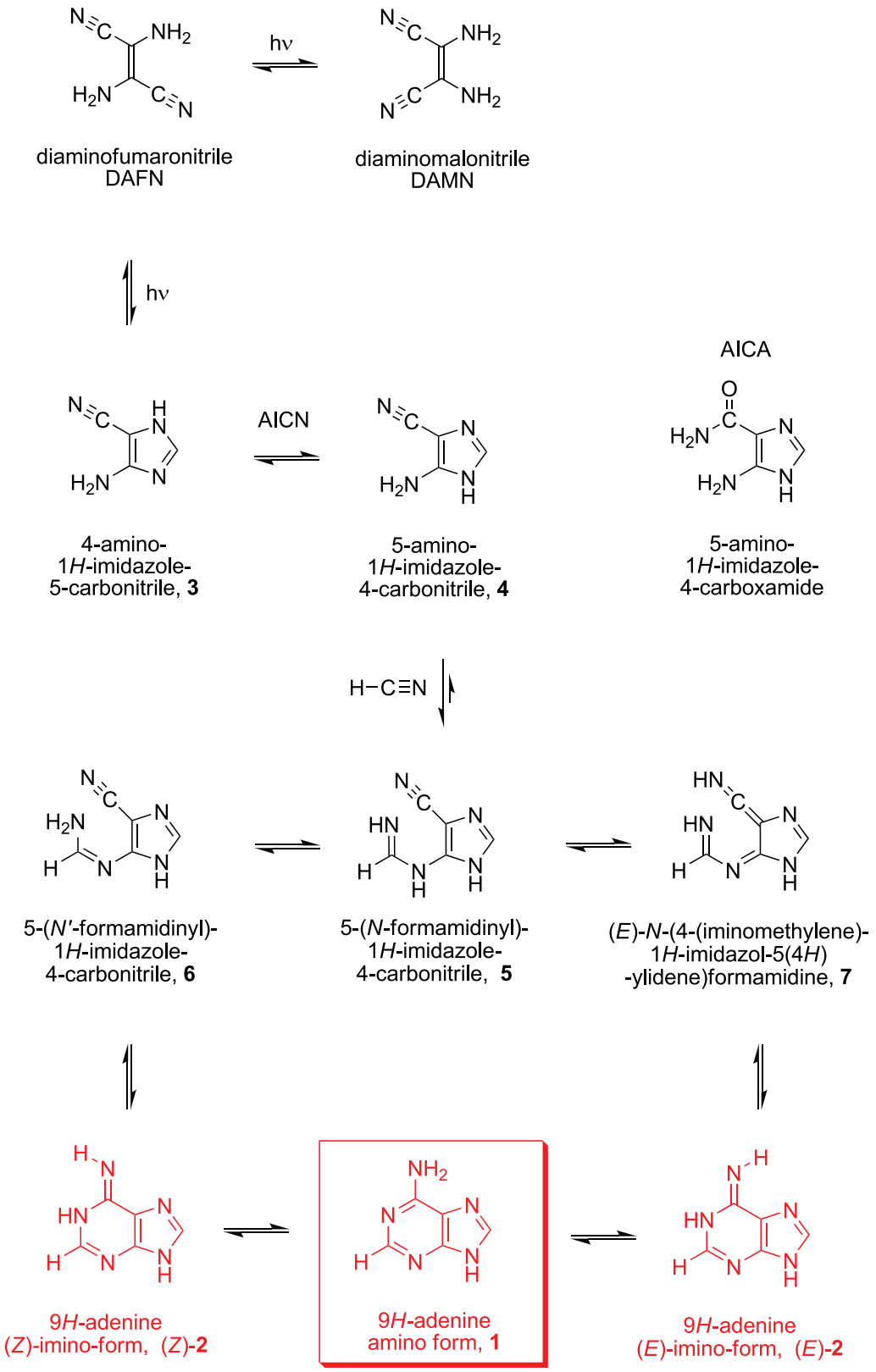

FIG. 1. Adenine formation from DAMN and DAFN via AICN.

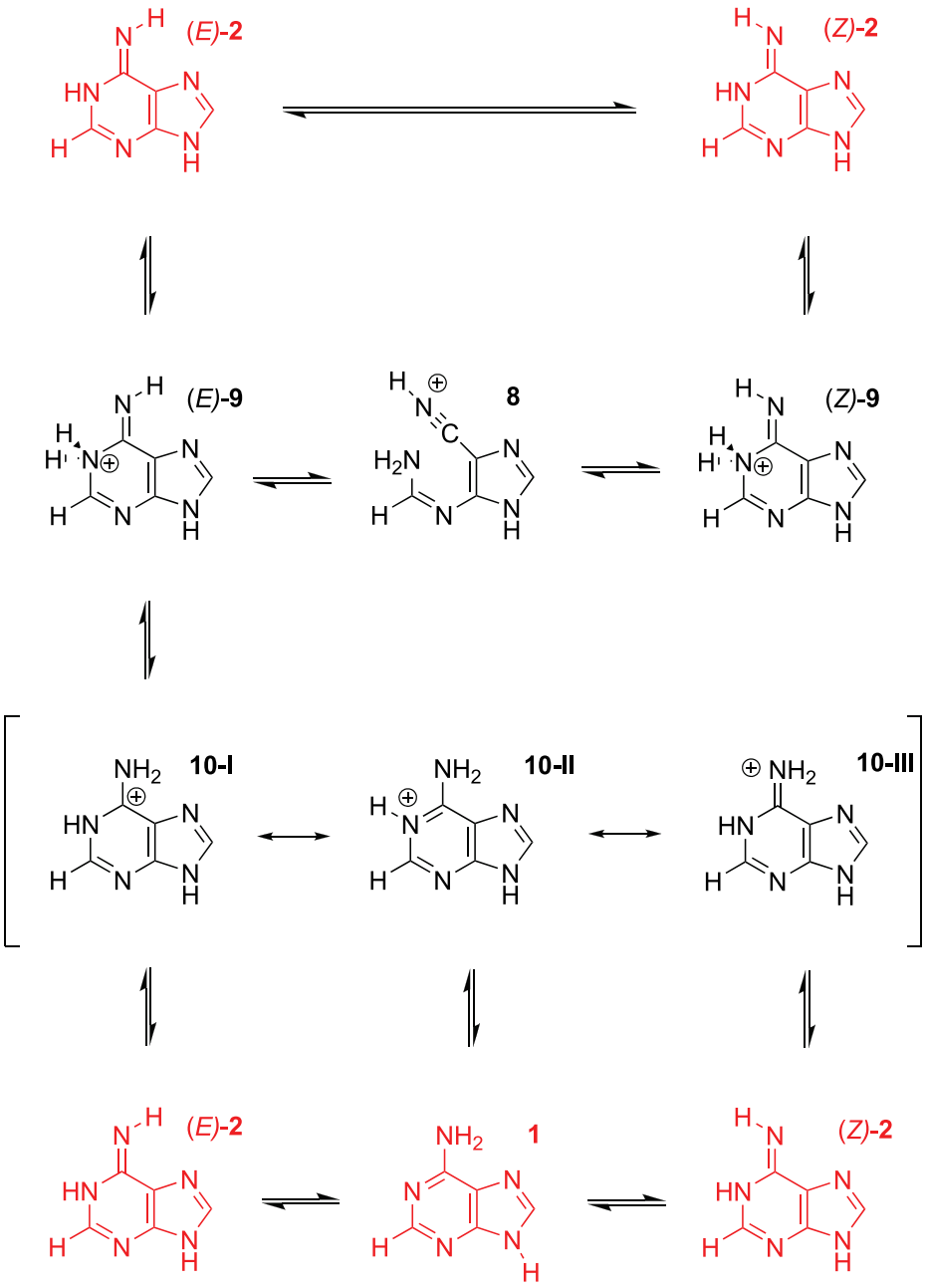

FIG. 2. Proton-catalyzed adenine formation from 5-(*N′*-formamidinyl)-1*H*-imidazole-4-carbonitrile 6.

with neutral nucleophiles require high activation energies. This is well known for nitrile hydrolysis, and the same applies to nitrile aminolysis (Wu and Glaser, 2005). The proton affinities of nitriles greatly exceed those of amines; thus, acid catalysis can provide for an efficient addition of amines to nitrilium ions. Hence, we studied the cyclization of **8** (:= [**6**+$\mathbf{H}^+$]) → **9** (:= [**2**+$\mathbf{H}^+$]). Next, we discuss pentamer **7** and its cyclization reaction **7** → **2**. N-imine protonation of **7**, should it occur, would result in **8** and its reaction to **9**. Interestingly, however, and potentially far more significant, we have discovered that the *uncatalyzed* reaction **7** → **2** is not only kinetically possible (while the uncatalyzed reaction **6** → **2** is not) but also proceeds practically without activation energy as soon as **7** is formed. With the reaction **6** → **2** possible and the reaction **7** → **2** inevitable via thermal paths, the most likely path from **5** to **2** depends on the availabilities of **6** and **7**. Hence, we

will discuss the thermodynamic preferences of the monocyclic pentamers **5**–**7** and the likelihood of their thermal and photolytic formations.

THEORETICAL METHODS AND COMPUTATIONS

All structures were fully optimized, and vibrational analyses were performed using second-order Møller-Plesset perturbation theory, MP2(full), with the 6-31G** basis set. The 6-31G** basis set is widely used in the chemistry community because it succeeds in reproducing experimental data with high reliability. The performance of these methods has been well established over many years (Cramer, 2002). Calculations were carried out with Gaussian 03 (Frisch *et al.*, 2003) on two clusters of Compaq alphaservers ES40 and ES45 and, more recently, with a 64-processor SGI Altix system. Total energies (E_{tot}), vibrational zero-point energies (*VZPE*), internal thermal energies (*TE*) due to rotation, vibration, and translation, and thermal entropies (*S*) are reported in Table 1.

Pertinent relative energies, activation barriers, and reaction energies are listed in Table 2. The energies ΔE refer to the static molecules at their optimized geometries, and energies ΔE_0 include vibrational zero-point energies, $\Delta E_0 = \Delta E + \Delta VZPE$. Vibrational frequencies are somewhat overestimated at the MP2(full)/6-31G** level. This overestimation can be corrected by appropriate scaling, *e.g.* the factor 0.9646 is recommended for use with MP2(full)/6-31G* data. While the scaling is important for the interpretation of IR spectra, scaling has hardly any consequences on relative energies, and we report relative energies that are based on the unscaled computed data. The enthalpies ($\Delta H_{298} = \Delta E + \Delta TE$) and Gibbs free energies ($\Delta G_{298} = \Delta H_{298} - T \cdot \Delta S$) listed in Table 2 were calculated at 298.15 K. In interstellar space, temperatures are around 2–10 K, and thus $\Delta E \approx \Delta E_0 \approx \Delta E_T \approx \Delta H_T \approx \Delta G_T$.

Animated gifs were created with the program Molekel (Portmann and Lüthi, 2000) to visualize atomic motions in the transition vectors associated with the transition states TS(**8**,(*E*)-**9**), TS(**8**,(*Z*)-**9**), and TS((*E*)-**9**,**10**). We have also created an animation of the rotational isomerization of **7** that leads to **2**. These animations can be viewed on the World Wide Web at http://web.missouri.edu/~glaserr/vitpub/PRC-animas/PRC-animas.html.

The photoexcitations were studied for conformers of **5** and the protonated pentamer **8** in several ways, including the configuration interaction methods CIS and CIS(D) (Foresman *et al.*, 1992; Head-Gordon *et al.*, 1994, 1995) the symmetry-adapted cluster CI method SAC-CI (Ehara

Table 1. Total Energies and Thermochemistry

Structure	E_{tot}[a,b]	*VZPE*[c]	TE_{298}[d]	S_{298}[e]	*NI*[f]
8	−466.331682	76.55	82.34	94.71	0
TS(**8**,(*E*)-**9**)	−466.309125	76.32	81.33	87.88	1
(*E*)-**9**	−466.327446	78.85	83.51	85.63	0
TS(**8**,(*Z*)-**9**)	−466.310756	76.71	81.54	87.07	1
(*Z*)-**9**	−466.312502	77.98	82.82	87.03	0
10	−466.414226	79.88	84.50	84.33	0
TS((*E*)-**9**,**10**)	−466.286989	75.93	80.27	83.01	1
5a	−465.997526	68.95	74.41	92.52	0
5b	−465.985783	68.21	74.23	95.02	0
6a	−465.997980	68.99	74.52	93.78	0
7b	−465.918869	67.53	75.12	94.52	0
7c	−465.918303	67.39	73.01	94.41	0
(*Z*)-**2** = "**7a**"	−466.005515	70.72	75.22	84.08	0
(*E*)-**2**	−466.016326	71.13	75.58	83.80	0
1	−466.036021	71.05	75.59	83.86	0

[a]All data computed at MP2(full)/6-31G**.
[b]Total energy (E_{tot}) in atomic units.
[c,d]Vibrational zero-point energies (*VZPE*, unscaled), and thermal energies (*TE*) in kilocalories per mole.
[e]Entropies (*S*) are in calories per mole and per Kelvin (cal $mol^{-1}K^{-1}$).
[f]Number of imaginary vibrational modes, *NI*.

Table 2. Relative Energies, Reaction Energies, and Activation Barriers[a]

Process	ΔE	ΔE_0	ΔH_{298}	ΔG_{298}
ΔE_A(**8** → TS(**8**, (*E*)-**9**))	14.16	13.92	13.14	15.18
ΔE_A((*E*)-**9** → TS(**8**,(*E*)-**9**))	11.50	8.97	9.32	8.65
ΔE_A(**8** → TS(**8**,(*Z*)-**9**))	13.13	13.29	12.33	14.61
ΔE_A((*Z*)-**9** → TS(**8**,(*Z*)-**9**))	1.10	−0.17	−0.18	−0.20
RE (**8** → (*E*)-**9**)	2.66	4.96	3.83	6.54
RE (**8** → (*Z*)-**9**)	12.04	13.47	12.52	14.81
ΔE_A((*E*)-**9** → TS((*E*)-**9**,**10**))	25.39	22.47	22.15	22.93
ΔE_A(**10** → TS((*E*)-**9**,**10**))	79.84	75.89	75.61	76.01
RE ((*E*)-**9** → **10**)	−54.46	−53.46	−53.47	−53.08
RE (**8** → **10**)	−51.80	−48.47	−49.64	−46.54
RE(**7b** → (*Z*)-**2**)	−54.37	−51.18	−54.27	−51.16
RE(**7b** → (*E*)-**2**	−61.16	−57.56	−60.70	−57.50
RE(**5a** → **5b**)	0.01	6.63	7.19	6.44
RE(**5a** → **6a**)	−0.28	−0.24	−0.17	−0.55
RE(**5b** → **6a**)	−7.65	−6.87	−7.36	−6.99
RE(**7b** → **7c**)	0.36	0.22	−1.75	−1.72
RE(**5a** → **7b**)	49.36	47.94	50.07	49.47
RE(**5b** → **7b**)	41.99	41.31	42.88	43.03
RE((*E*)-**2** → (*Z*)-**2**)	6.78	6.37	6.42	6.34
RE(**1** → (*E*)-**2**)	12.36	12.44	12.35	12.37
RE(**1** → (*Z*)-**2**)	19.14	18.81	18.77	18.71
RE(**1** → **5a**)	24.16	22.06	22.98	20.39
RE(**1** → **5b**)	31.52	28.68	30.16	26.84

[a]Relative energies computed at MP2(full)/6-31G** in kcal/mol.

et al., 2005) and time-dependent density functional theory, TD-DFT (Marques and Gross, 2004; Van Gisbergen and Baerends, 2004). The TD-DFT method was employed in conjunction with the hybrid density functional method B3LYP, TD-B3LYP (Chatgilialoglu *et al.*, 2006; Ljubic and Sabljic, 2006). The triply-split valence basis set 6-311G** was used in the calculations of excited states, and all of the computations of excited singlet states were based on the optimized ground state structures, *e.g.* method/6-311G**//MP2 (full)/6-31G**. Results are summarized in Table 3.

RESULTS

Pyrimidine-ring formation via proton-catalyzed nitrile-aminolysis

Nitrilium ion **8** results by cyano-N protonation of pentamer **6**. There are two paths for intramolecular C–N bond formation, and they lead to (*E*)-**9** and (*Z*)-**9**, respectively. The energy profiles for both paths are shown in Fig. 3, and molecular models of the transition state structures and of the products are shown in Fig. 4.

While the activation barriers of 13.1 and 12.3 kcal/mol are comparable for the reactions **8** → (*E*)-**9** and **8** → (*Z*)-**9**, respectively, the profiles are rather different. Isomer (*Z*)-**9** is less stable than (*E*)-**9**; hence, for (*Z*)-**9** there is hardly any barrier to back-reaction to **8**. In fact, with the consideration of the vibrational energies, the calculations suggest that (*Z*)-**9** does not correspond to a local minimum on the enthalpy and free energy surfaces. Product (*E*)-**9** is more interesting. The formation of (*E*)-**9** is only slightly endothermic, and there is a barrier to back-reaction so that (*E*)-**9** can have some lifetime.

The path **8** → **9** is an adenine synthesis only if (*E*)-**9** can be stabilized before it reacts back to **8**. One way to accomplish this consists in the intramolecular H-transfer (*E*)-**9** → **10**. This H-transfer was studied; molecular models of the transition state structure TS((*E*)-**9**,**10**) and of product **10** are shown in Fig. 4. The tautomerization requires an activation enthalpy of about 22.3 kcal/mol and is exothermic by 53.5 kcal/mol. Thus, this second step makes the overall reaction of **8** → (*E*)-**9** → **10** exothermic by 48.5 kcal/mol.

These paths were discussed recently as part of a mass-spectrometric study of protonated adenine (Turecek and Chen, 2005). Using the B3-MP2

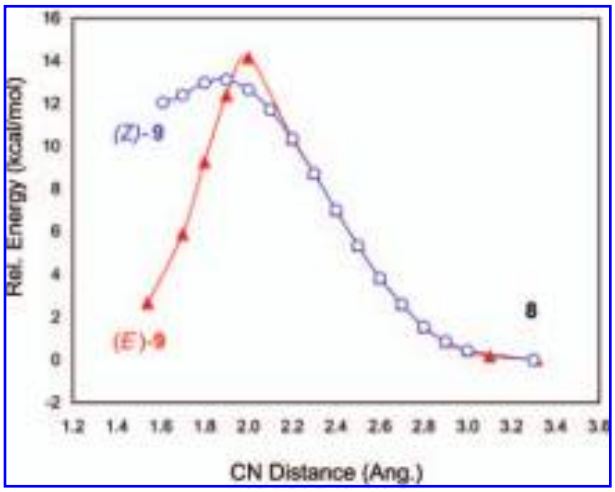

FIG. 3. Reaction paths for the cyclizations of 8 to (*E*)-9 and (*Z*)-9.

scheme, the authors computed activation barriers of 16.3 and 16.7 kcal/mol for the reactions **8** → (*E*)-**9** and **8** → (*Z*)-**9**, respectively, and an activation barrier for the H-transfer of 22.5 kcal/mol.

The effectiveness of the proton-catalyzed path to adenine depends on the ratio between the back-reaction of (*E*)-**9** and the less facile H-transfer. The first step of the reaction sequence **8** → (*E*)-**9** → **10** might set up an internal motion so that the subsequent H-transfer is hard to avoid. Animations of the intrinsic reaction paths of both steps strongly suggest this possibility, and a dynamic study might be of interest to examine this point. Yet even under the very best conditions, it becomes clear that the total energy required to overcome the barriers of the reaction sequence **8** → (*E*)-**9** → **10** far exceeds the thermal energy available in interstellar space.

Uncatalyzed cyclization of the monocyclic HCN-pentamer

We have determined the structures of the monocyclic HCN pentamers **5** to **7** and of the purines **1** and **2** shown in Fig. 5. The computed results are included in Tables 1 and 2, and molecular models of the equilibrium structures are shown in Fig. 6.

Pentamer **7** can form geometrical isomers about the exocyclic C=N bond as well as about the formamidine C=NH bond. We are primarily interested in (*E,E*)-**7** because this isomer can cyclize; we refer to that isomer simply as **7** (Fig. 5). Molecule **7** can form rotamers about the C–N bond of the diazabutadiene system, and a cisoid conformation is required for the imine-NH to approach the keteneimine. We searched for such a cisoid structure of **7a**, but all these attempts resulted directly in (*Z*)-**2**.

A scan of the potential energy surface of **7** as a function of the ∠(HN=CH–N=C) dihedral angle τ resulted in the plots of Fig. 7. There is some interesting detail in the flat region ($60° < \tau < 300°$), which contains the minima **7b** and **7c**, but the striking messages of Fig. 7 are that the cyclization **7** → (*Z*)-**2** is highly exothermic and the cyclization proceeds essentially without any activation energy. Merely a rotation about the C–N bond is required for **7b** or **7c** to form the purine skeleton, and there is always enough internal energy to accomplish such an internal rotation no matter what the temperature: $VZPE(\mathbf{7}) > 65$ kcal/mol (Table 1).

We studied this cyclization starting from minima **7b** and **7c** and found that both initial structures lead to (*Z*)-**2** via their respective least-motion paths. This stereoselectivity occurs because pyrimidine formation involves essentially complete coplanarization of the amidine side chain with the plane of the imidazole. When such a **7a**-like structure is reached along either one of the reaction paths, only then will the keteneimine moiety bend, and its keteneimine-H will begin to move toward its position in (*Z*)-**2**.

The absence of an activation barrier for the cyclization **7** → (*Z*)-**2** can be explained with dative bonding theory (Hodgen *et al.*, 2003) and, formally, with the theory of pericyclic reactions (Tantillo, 2006; Morgan, 2005). In the dative bonding model, the new C-N σ-bond is formed by shifting the imine's N-lone pair toward the central C-atom of the keteneimine. If this dative bond formation were the only event, it would lead to charge transfer and charge separation. Yet it is the key feature of the reaction **7** → **2** that the charge transfer associated with the σ-bond's formation can occur *without overall charge separation*. Imines are highly polar, and the positive charge of the imine's carbon can be delocalized in the π-system as shown by the polar resonance form (Fig. 5, bottom). The N → C dative bond formation and this polarization in the pseudo-π-system shift electron density in *opposite* directions. Hence, the cyclization via N → C dative bond formation becomes possible and indeed proceeds essentially without activation barrier because it can proceed without significant charge separation. The reaction **7** → **2** formally qualifies as heteroanalogue of

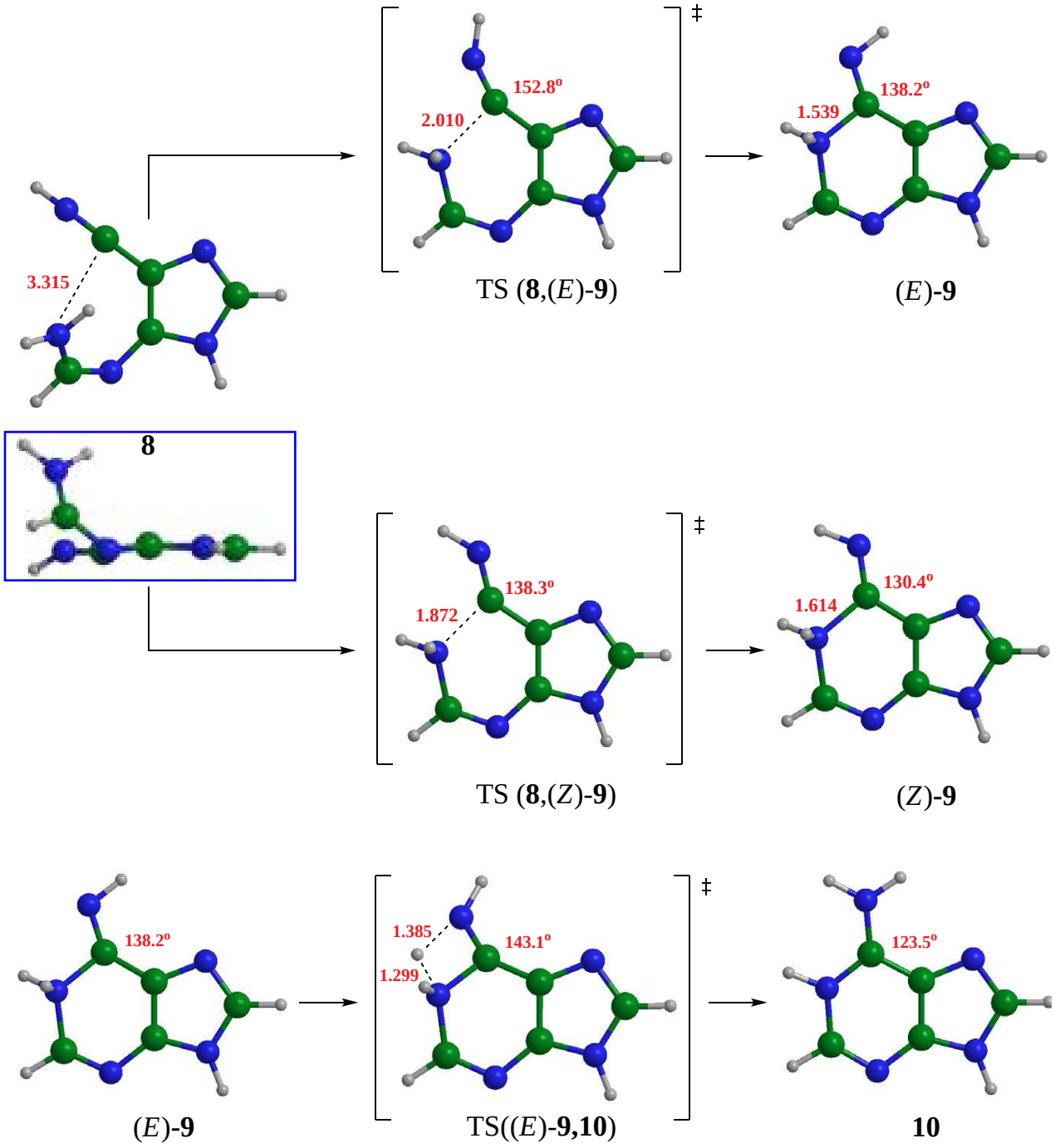

FIG. 4. Molecular models of the stationary structures along the paths of 8 → **TS(**8,**(*E*)-**9**)** → **(*E*)-**9 **and** 8 → **TS(**8,**(*Z*)-**9**)** → **(*Z*)-**9 **(top), and along the path of (*E*)-**9 → **TS((*E*)-**9,10**)** → 10.

the electrocyclization of 1,3,5-hexatriene (Chuang and Zare, 1985) and more precisely of a (Z)-hepta-1,2,4,6-tetraene. However, genuine pericyclic reactions involve transition states with overlap between the (slightly distorted) π-systems of the termini of the 1,3,5-triene, and their structures are characterized by conrotatory or disrotatory torsions of the terminal moieties. The pyrimidine formation in the reaction **7** → **2** proceeds with essentially complete coplanarization of the amidine side chain with the plane of the imidazole (see above), and the reaction paths do not show the torsions that would be typical along the paths of pericyclic reactions. The term "pseudopericyclic

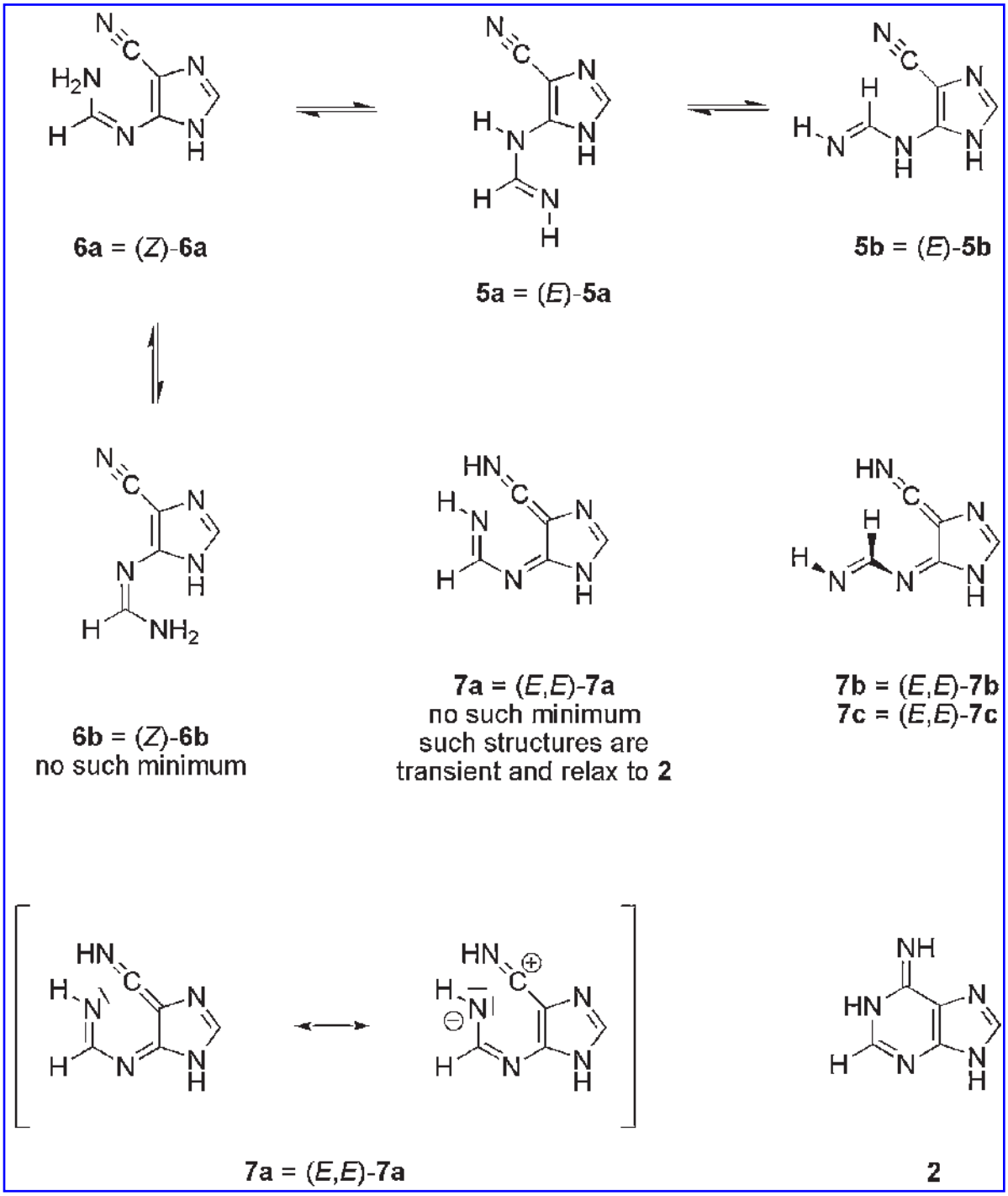

FIG. 5. Rotamers of monocyclic HCN-pentamers 5–7. Only those geometrical isomers are shown that allow for pyrimidine formation.

reaction" has been suggested for reactions of this type (Morgan, 2005).

Photoactivation of pyrimidine cyclization

We have identified two potential paths for pyrimidine-ring formation of the monocyclic HCN pentamer; these are the proton-catalyzed intramolecular nitrile aminolysis **8** → (*E*)-**9** → **10** and the uncatalyzed cyclization **7** → (*Z*)-**2**. While starting material **8** is available by protonation of **5**, the thermal reaction along this cyclization path is frustrated by high barriers. On the other hand, the second path is frustrated by the thermal non-

Table 3. Electronic Excitations

Method[a]	Molecule	Excitation Energy and Wavelength			Oscillator strength, *f*
		ΔE(eV)	ΔE(kcal/mol)	λ_{max}(nm)	
CIS	**5a**	6.030	139.1	205.6	0.493
		6.086	140.3	203.7	0.000
		7.124	164.3	174.0	0.142
	5b	6.246	144.0	198.5	0.245
		6.342	146.2	195.5	0.001
		7.006	161.6	177.0	0.004
	8	5.121	118.1	242.1	0.176
		5.200	119.9	238.5	0.157
		6.705	154.6	184.8	0.028
CIS(D)[b]	**5a**	5.736	132.3	216.1	
		6.945	160.2	178.5	
		7.108	163.9	174.4	
	5b	6.420	148.0	193.1	
		7.452	171.8	166.4	
		8.081	186.3	153.4	
	8	4.371	100.8	283.7	
		4.529	104.4	273.7	
		5.088	117.3	243.7	
SAC-CI	**5a**	6.549	151.0	189.3	0.000
		6.660	153.6	186.2	0.195
		7.860	181.3	157.7	0.003
	5b	5.948	137.2	208.5	0.291
		6.791	156.6	182.6	0.003
		7.508	173.1	165.1	0.015
	8	4.186	96.5	296.2	0.205
		4.325	99.7	186.6	0.047
		5.429	125.2	228.4	0.063
TD-B3LYP	**5a**	4.803	110.8	258.1	0.371
		5.309	122.4	233.5	0.000
		5.714	131.8	217.0	0.000
	5b	5.063	116.8	244.9	0.153
		5.700	131.4	217.5	0.035
		5.842	134.7	212.2	0.016
	8	3.719	85.8	333.4	0.006
		3.893	89.8	318.5	0.130
		4.337	100.0	285.9	0.015

[a]For each method, the theoretical level was method/6-311G**//MP2(full)/6-31G**.
[b]Oscillator strength for CIS(D) values is not available.

accessibility of **7** due to its high energy relative to **5**. Pentamer **5** is over 40 kcal/mol more stable than **7**, and there clearly is no thermal path from **5** to **7** in interstellar space. Here we show that both of these cyclization paths can be photoactivated. We computed the three lowest excited singlet states of **5** and **8**, the results of which are listed in Table 3.

Several theoretical methods were employed, and we comment briefly on their performances with regard to the predicted excitation energies and the intensities of the absorptions. For **5a** and **5b**, the traditional methods CIS and CIS(D) and the considerably more sophisticated SAC-CI method yield excitation energies that agree within 15 nm, but the intensities can differ by magnitudes. The results for **8** differ more drastically in that the CIS and CIS(D) methods suggest near-degenerate absorptions, whereas SAC-CI shows just one strong absorption at much lower energy. The TD-DFT approach, unfortunately, does not present itself as an alternative for the present task. Compared to the SAC-CI data, TD-B3LYP results significantly underestimate the excitation energies and give erroneous estimates of their intensity ratio. It is for these reasons that it was deemed necessary to perform the computer-time-demanding SAC-CI calculations (several days of CPU time for each molecule), the results of which are discussed below.

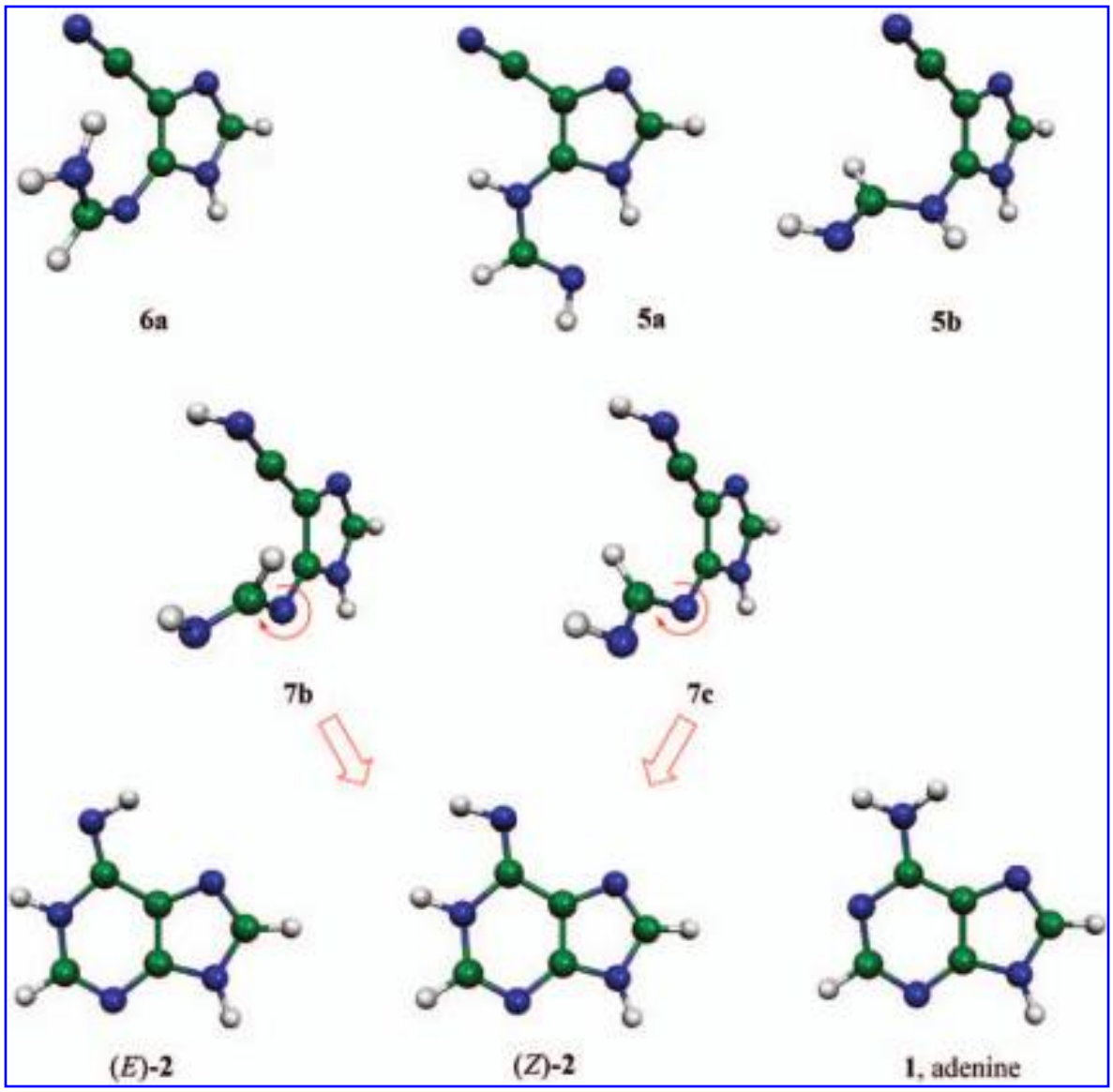

FIG. 6. Molecular models of monocyclic and bicyclic HCN-pentamers: Formamidines 6a, 5a **and** 5b **(top row), keteneimines** 7b **and** 7c **(center row), and pentamers (*E*)-**2**, (*Z*)-**2**, and adenine** 1 **itself.**

The photoexcitation of the neutral HCN-pentamers **5a** and **5b**, respectively, requires light with wavelengths below 189 and 209 nm, respectively. Photoexcited **5*** contains over 135 kcal/mol of additional internal energy and has the capacity to tautomerize to **7**. Pentamer **5** absorbs in the UV-C range (<280 nm), and none of the Sun's UV-C light reaches even the Earth's stratosphere. It is safe to extrapolate this conclusion to condensed-phase situations on Earth because it would be difficult to argue for a bathochromic shift into the UV-B range. On the other hand, the absorbance of **5** occurs well within the intense region of the local interstellar UV radiation field (Henry, 2002; Sujatha *et al.*, 2004) and the young Earth was exposed to significant UV-C radiation (3.1 W/m^2) (Buccino *et al.*, 2004).

The photoexcitation of **8** requires light with wavelengths below 296 nm, and this absorption appears on the high-energy side of the UV-B range. Molecular oxygen and stratospheric ozone prevent most, but not all, of the UV-B radiation from reaching the surface of the modern Earth (*circa* 4 W/m^2; Rozema *et al.*, 2002), and the UV-B intensity on the surface of the young Earth (*circa* 12 W/m^2) was about three times higher (Buccino *et al.*, 2004).

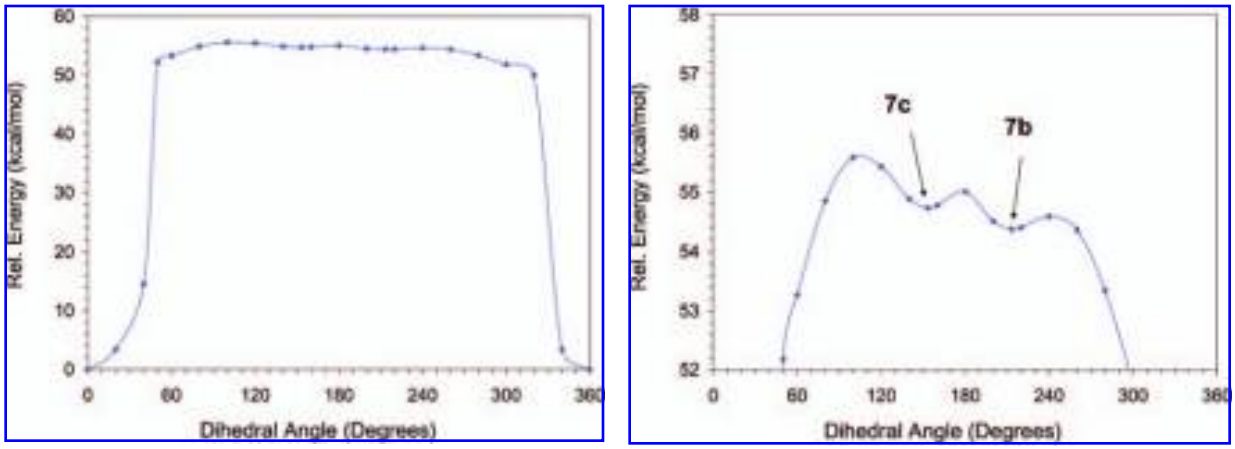

FIG. 7. Potential energy surface of 7 as a function of the HN=CH–N=C dihedral angle and relative to (*Z*)-2.

DISCUSSION

The significance of the results presented is discussed with reference to Fig. 8. This figure schematically shows important areas of the potential energy surfaces (PES) of neutral and protonated HCN-pentamer. The potential energy diagram is drawn to scale with regard to the vertical energy axis, and the PES regions of $(HCN)_5$ and $H^+(HCN)_5$ are connected by the experimental proton affinity of 236 kcal/mol of adenine (Greco *et al.*, 1990; Liguori *et al.*, 2000). Protonation/deprotonation and deprotonation/reprotonation sequences provide for tautomerizations of $(HCN)_5$ and $H^+(HCN)_5$, respectively. In condensed phase these equilibria are fast; however, in the cold vacuum of interstellar space they are very slow if they occur at all.

Adenine is the "thermodynamic sink" for $(HCN)_5$, and the same is true for the protonated system $H^+(HCN)_5$. Protonated adenine **10** is more stable than **8**; the computed difference in their stabilities is so large that it is entirely safe to say that none of the protonated monocyclic pentamers come close to **10** (and isomers of **8** would be expected to be less stable than **8**). Hence, adenine **1** will be formed from **5** given enough time, suitable reaction channels, and sources of sufficient activation energy to access these channels. The reaction of AICN with HCN or $[HCNH]^+$ yields **5** directly or after deprotonation. There is no direct reaction channel from amidine **5** to adenine **1**.

In a proton-rich environment, the isomerization between the nearly isoenergetic pentamers **5** and **6** becomes a reaction channel, and protonated derivatives of **5** and **6** become potential substrates. Our results suggest that **8** requires about 30 kcal/mol of activation energy for *thermal* pyrimidine formation. While this path is not likely in interstellar space, the conditions employed in the experiments by Zubay and Mui (2001) and by Hill and Orgel (2002) make this path thermally accessible. Alternatively, this reaction path might be followed after photoactivation of **8**. The computed excitation characteristics of **8** suggest that the channel for photolytic reaction is open in interstellar space and on Earth (early and modern).

In the absence of protons, only pentamer **7** offers a reaction channel to the purine system. Pentamer **5** might rely on hydrogen-tunneling (Arnaut *et al.*, 2006) to isomerize to **6**, but the endothermicity of the isomerization of **5** to **7** excludes any low-temperature path. This isomerization can only be accomplished with photoactivation. The computed excitation characteristics of **5a** and **5b** suggest that this channel is open in interstellar space and that it might have been accessible on early Earth as well.

CONCLUSION

One of the major goals of prebiotic chemistry is the search for possible syntheses of the nucleobases and especially of the purine bases (Levy and Miller, 1999). Building on the results of half a century of studies of adenine synthesis by HCN pentamerization, we have discussed mechanisms

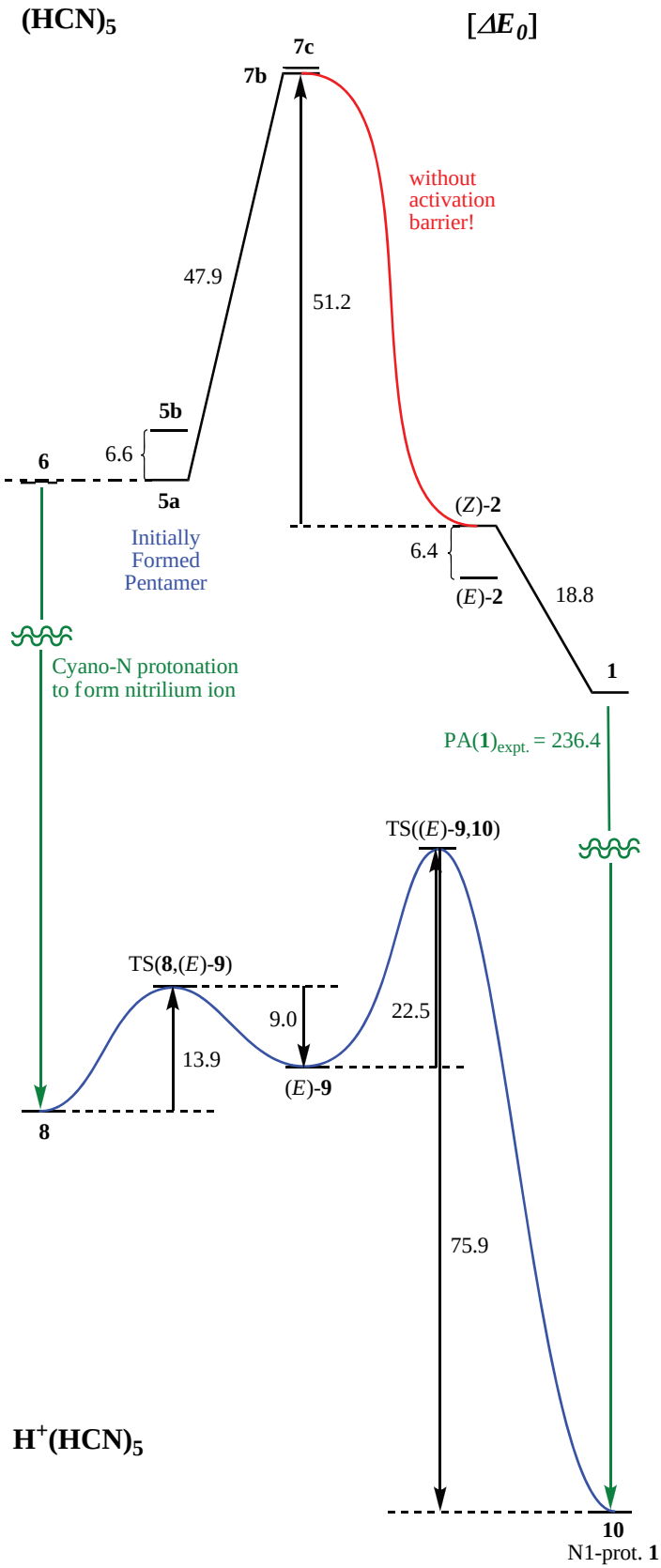

FIG. 8. Schematic illustrations of sections of the potential energy surfaces of HCN pentamer and of protonated HCN-pentamer, respectively, relevant to prebiotic adenine synthesis.

for possible prebiotic pyrimidine-ring formation of monocyclic HCN-pentamers. The calculations model gas-phase chemistry, and the results primarily inform discussions of adenine synthesis in interstellar space. The primary conclusions are (a) that 5-(*N'*-formamidinyl)-1*H*-imidazole-4-carbonitrile, **6**, can serve as a substrate for *proton-catalyzed* purine formation under photolytic conditions and (b) that *N*-(4-(iminomethylene)-1*H*-imidazol-5(4*H*)-ylidene)formamidine, **7**, can serve as a substrate for *uncatalyzed* purine formation under photolytic conditions.

Photoexcitation of the initially formed monocyclic HCN-pentamer 5-(*N*-formamidinyl)-1*H*-imidazole-4-carbonitrile, **5**, provides more than 135 kcal/mol of additional internal energy to **5***. Tautomerization to **7** would convert about one third of the excess internal energy into electronic energy and leave the nascent isomer **7** with just about twice its normal internal energy. Such an isomer **7** might be cool enough to prevent any dissociations, while IR fluorescence dissipates the excess energy. The absence of any sizeable activation barrier for the cyclization **7** → (*Z*)-**2** is remarkable, and it is this feature that allows for the formation of the purine skeleton from **7** without any further activation. The exploration of this chemistry presents a considerable challenge for synthetic chemistry.

ACKNOWLEDGMENTS

This research was supported in part by the MU Research Board (RB #2358) and the National Institutes of Health (GM61027). We gratefully acknowledge support of MU Research Computing by Federal Earmark NASA Funds for Bioinformatics Consortium Equipment and additional financial support from Dell, SGI, Sun Microsystems, TimeLogic, and Intel.

SUPPORTING INFORMATION AVAILABLE

Cartesian coordinates and Chime displays of optimized structures, and animations of reaction paths are available directly from the authors and can be viewed online at the author's web site at http://web.missouri.edu/~glaserr/vitpub/PRC-animas/PRC-animas.html.

REFERENCES

Arnaut, L.G., Formosinho, S.J., and Barroso, M. (2006) Tunnelling in low-temperature hydrogen-atom and proton transfers. *J. Mol. Struct.* 786, 207–214.

Borquez, E., Cleaves, H.J., Lazcano, A., and Miller, S.L. (2005) An investigation of prebiotic purine synthesis from the hydrolysis of HCN polymers. *Orig. Life Evol. Biosph.* 35, 79–90.

Buccino, A.P., Mauas, P.J.D., and Lemarchand, G.A. (2004) UV radiation in different stellar systems. In *Bioastronomy 2002: Life Among the Stars, IAU Symposium 213*, edited by R.P Norris and F.H. Stootman, Astronomical Society of the Pacific, San Francisco, pp. 97–100.

Chatgilialoglu, C., Caminal, C., Altieri, A., Vougioukalakis, G.C., Mulazzani, Q.G., Gimisis, T., and Guerra, M. (2006) Tautomerism in the guanyl radical. *J. Am. Chem. Soc.* 128, 13796–13805.

Chuang, M.C. and Zare, R.N. (1985) Evidence for inhomogeneous broadening in vibrational overtone transitions: formation of 1,3-cyclohexadiene from cis-1,3,5-hexatriene. *J. Chem. Phys.* 82, 4791–4801.

Chyba, C. and Sagan, C. (1992) Endogenous production, exogenous delivery and impact-shock synthesis of organic molecules: an inventory for the origins of life. *Nature* 355, 125–132.

Cramer, C. J. (2002) *Essentials of Computational Chemistry: Theories and Models*, John Wiley and Sons, New York.

Ehara, M., Hasegawa, J., and Nakatsuji, H. (2005) SAC-CI method applied to molecular spectroscopy. In *Theory and Applications of Computational Chemistry: The First Forty Years*, edited by C.E. Dykstra, Elsevier B.V., Amsterdam, the Netherlands, pp. 1099–1141.

Ferris, J.P. and Orgel, L.E. (1966) Studies on prebiotic synthesis. I. Aminomalononitrile and 4-amino-5-cyanoimidazole. *J. Am. Chem. Soc.* 88, 3829–3831.

Foresman, J.B., Head-Gordon, M., Pople, J.A., and Frisch, M.J. (1992) Toward a systematic molecular orbital theory for excited states. *J. Phys. Chem.* 96, 135–149.

Frisch, M.J., Trucks, G.W., Schlegel, H.B., Scuseria, G.E., Robb, M.A., Cheeseman, J.R., Montgomery, Jr., J.A., Vreven T., Kudin, K.N., Burant, J.C., Millam, J.M., Iyenger, S.S., Tomasi, J., Barone, V., Mennucci, B., Cossi, M., Scalmani, G., Rega, N., Petersson G.A., Nakatsuji, H., Hada, M., Ehara, M., Toyota, K., Fukuda, R., Hasegawa, J., Ishida, M., Nakajima, T., Honda, Y., Kitao, O., Nakai, H., Klene, M., Li, X., Knox, J.E., Hratchian, H.P., Cross, J.B., Adamo, C., Jaramillo, J., Gomperts, R., Stratmann, R.E., Yazyev, O., Austin, A.J., Cammi, R., Pomelli, C., Ochterski, J.W., Ayala, P.Y., Morokuma, K., Voth, G.A., Salvador, P., Dannenberg, J.J., Zakrzewski, V.G., Dapprich, S., Daniels, A.D., Strain M.C., Farkas, O., Malick, D.K., Rabuck A.D., Raghavachari, K., Foresman, J.B., Ortiz, J.V., Cui, Q., Baboul, A.G., Clifford, S., Cioslowski, J., Stefanov, B.B., Liu, G., Liashenko, A., Piskorz, P., Komaromi, I., Martin, R.L., Fox, D.J., Keith, T., Al-Laham, M.A., Peng, C.Y., Nanavakkara, A., Challacombe, M., Gill, P.M.W., Johnson, B., Chen, W., Wong, M.W., Gonzalez, C.,

Pople, J.A. (2003) *Gaussian 03, Revision A.1*, Gaussian Inc., Pittsburgh.

Ghosh, K.K. and Ghosh, S.N. (1980) A mechanism for the formation of glycine, adenine and guanine in interstellar space. *Life Sci. Space Res.* 18, 37–42.

Ghosh, S.N. and Ghosh, K.K. (1982) Rate coefficients of some important interstellar ion-neutral reactions. *Indian J. Radio Space Phys.* 11, 40–41.

Greco, F., Liguori, A., Sindona, G., and Uccella, N. (1990) Gas-phase proton affinity of deoxyribonucleosides and related nucleobases by fast atom bombardment tandem mass spectrometry. *J. Am. Chem. Soc*. 112, 9092–9096.

Habicht, K.S., Gade, M., Thamdrup, B., Berg, P., and Canfield, D.E. (2002) Calibration of sulfate levels in the Archean Ocean. *Science* 298, 2372–2374.

Head-Gordon, M., Rico, R.J., Oumi, M., and Lee, T.J. (1994) A doubles correction to electronic excited states from configuration interaction in the space of single substitutions. *Chem. Phys. Lett.* 219, 21–29.

Head-Gordon, M., Maurice, D., and Oumi, M. (1995) A perturbative correction to restricted open shell configuration interaction with single substitutions for excited states of radicals. *Chem. Phys. Lett.* 246, 114–121.

Henry, R.C. (2002) The local interstellar ultraviolet radiation field. *Astrophys. J.* 570, 697–707.

Hill, A. and Orgel, L.E. (2002) Synthesis of adenine from HCN tetramer and ammonium formate. *Orig. Life Evol. Biosph.* 32, 99–102.

Hodgen, B., Rayat, S., and Glaser, R. (2003) Nitrosative adenine deamination: facile pyrimidine-ring opening in the dediazoniation of adeninediazonium ion. *Org. Lett.* 5, 4077–4080.

Ishii, K., Tajima, A., Taketsugu, T., and Yamashita, K. (2006) Theoretical elucidation of the unusually high [HNC]/[HCN] abundance ratio in interstellar space: two-dimensional and two-state quantum wave packet dynamics study on the branching ratio of the dissociative recombination reaction $HCNH^+ + e^- \rightarrow$ HNC/HCN + H. *Astrophys. J.* 636, 927–931.

Kissel, J., and Krueger, F.R. (1987) The organic component in dust from comet Halley as measured by the PUMA mass spectrometer on board Vega 1. *Nature* 326, 755–760.

Kliss, R.M. and Matthews, C.N. (1962) Hydrogen cyanide dimer and chemical evolutions. *Proc. Natl. Acad. Sci. U.S.A.* 48, 1300–1306.

Levy, M. and Miller, S.L. (1999) The prebiotic synthesis of modified purines and their potential role in the RNA world. *J. Mol. Evol.* 48, 631–637.

Levy, M., Miller, S.L., Brinton, K., and Bada, J.L. (2000) Prebiotic synthesis of adenine and amino acids under Europa-like conditions. *Icarus* 145, 609–613.

Liguori, A., Napoli, A., and Sindona, G. (2000) Survey of the proton affinities of adenine, cytosine, thymine and uracil dideoxyribonucleosides, deoxyribonucleosides and ribonucleosides. *J. Mass Spectrom*. 35, 139–144.

Ljubic, I. and Sabljic, A. (2006) Theoretical study of structure, vibrational frequencies, and electronic spectra of polychlorinated dibenzo-p-dioxins. *J. Phys. Chem. A Mol. Spectrosc. Kinet. Environ. Gen. Theory* 110, 4524–4534.

Marques, M.A.L. and Gross, E.K.U. (2004) Time-dependent density functional theory. *Ann. Rev. Phys. Chem.* 55, 427–455.

Matthews, C.N. (1997) Hydrogen cyanide polymers from the impact of comet P/Shoemaker-Levy 9 on Jupiter. *Adv. Space Res.* 19, 1087–1091.

Miller, S.L. and Urey, H.C. (1959) Organic compound synthesis on the primitive Earth. Several questions about the origin of life have been answered, but much remains to be studied. *Science* 130, 245–51.

Morgan, K.M. (2005) Reaction mechanisms. Part (iii) pericyclic reactions. *Ann. Rep. Prog. Chem. Sect. B* 101, 284–304.

Orgel, L.E. (2004) Prebiotic adenine revisited: eutectics and photochemistry. *Orig. Life Evol. Biosph*. 34, 361–369.

Oro, J. (1961) Mechanism of synthesis of adenine from hydrogen cyanide under possible primitive earth conditions. *Nature* 191, 1193–1194.

Oro, J. and Kimball, A.P. (1962) Synthesis of purines under possible primitive earth conditions. II. Purine intermediates from hydrogen cyanide. *Arch. Biochem. Biophys*. 96, 293–313.

Penfold, B.R. and Lipscomb, W.N. (1961) The molecular and crystal structure of hydrogen cyanide tetramer (diaminomaleonitrile). *Acta Crystallograph. Sect. F Struct. Biol. Cryst. Commun.* 14, 589–597.

Plese, M. and Jasien, P.G. (1996) The photochemical isomerization of DAMN to ACI: stability of potential intermediates. *J. Mol. Struct.* 364, 121–130.

Ponnamperuma, C., Lemmon, R.M., Mariner, R., and Calvin, M. (1963) Formation of adenine by electron irradiation of methane, ammonia, and water. *Proc. Natl. Acad. Sci. U.S.A.* 49, 737–740.

Portmann, S. and Lüthi, H.P. (2000) Molekel: an interactive molecular graphics tool. *Chimia* 54, 766–770.

Rozema, J., Geel, B.V., Björn, L.O., Lean, J., and Madronich, S. (2002) Toward solving the UV puzzle. *Science* 296, 1621–1622.

Sanchez, R., Ferris, J.P., and Orgel, L.E. (1966) Conditions for purine synthesis: Did prebiotic synthesis occur at low temperatures? *Science* 153, 72–73.

Sanchez, R.A., Ferris, J.P., and Orgel, L.E. (1967) Studies in prebiotic synthesis II. Synthesis of purine precursors and amino acids from aqueous hydrogen cyanide. *J. Mol. Biol.* 30, 223–253.

Sanchez, R.A., Ferris, J.P., and Orgel, L.E. (1968) Studies in prebiotic synthesis IV. Conversion of 4-aminoimidazole-5-carbonitrile derivatives to purines. *J. Mol. Biol.* 38, 121–128.

Schwartz, A.W., Joosten, H., and Voet, A.B. (1982) Prebiotic adenine synthesis via HCN oligomerization in ice. *BioSystems* 15, 191–193.

Shapiro, R. (1995) The prebiotic role of adenine: a critical analysis. *Orig. Life Evol. Biosph.* 25, 83–98.

Smith, I.W.M., Talbi, D., and Herbst, E. (2001) The production of HCN dimer and more complex oligomers in dense interstellar clouds. *Astron. Astrophys*. 369, 611–615.

Sujatha, N.V., Chakraborty, P., Murthy, J., and Henry, R.C. (2004) A model of the stellar radiation field in the UV. *Bulletin of the Astronomical Society of India* 32, 151–158.

Tantillo, D.J. (2006) Reaction mechanisms. Part (ii). Pericyclic reactions. *Annu. Rep. Prog. Chem. Sect. B*. 102, 269–289.

Tennekes, P.P., Harju, J., Juvela, M., and Toth, L.V. (2006) HCN and HNC mapping of the protostellar core Chameleon-MMS1. *Astron. Astrophys*. 456, 1037–1043.

Tian, F., Toon, O.B., Pavlov, A.A., and De Sterck, H. (2005) A hydrogen-rich early Earth atmosphere. *Science* 308, 1014–1017.

Turecek, F. and Chen, X. (2005) Protonated adenine: tautomers, solvated clusters, and dissociation mechanisms. *J. Am. Soc. Mass Spectrom.* 16, 1713–1726.

Van Gisbergen, S.J.A. and Baerends, E.J. (2004) Time-dependent density functional resonance theory. In *Comprehensive Coordination Chemistry II*, edited by J.A. McCleverty and T.J. Meyer, Elsevier Ltd., Oxford, 2, 511–517.

Wu, H. and Glaser, R. (2005) Amino-effect on the protonation of beta-aminoacrylonitrile. *Chem. Res. Toxicol*. 18, 111–114.

Yamada, Y., Nagashima, N., Iwashita, Y., Nakamura, A., and Kumashiro, I. (1968) The synthesis and the molecular structure of diaminofumaronitrile. *Tetrahedron Lett.* 43, 4529–4532.

Zubay, G. and Mui, T. (2001) Prebiotic synthesis of nucleotides. *Orig. Life Evol. Biosph.* 31, 87–102.

Address reprint requests to:
Rainer Glaser
Department of Chemistry
321 Chemistry Building
601 South College Avenue
University of Missouri-Columbia
Columbia, Missouri 65211

E-mail: glaserr@missouri.edu